Homogeneous observer for a low-dimensional neural fields model of cortical activity

A.M. Annabi, L. Sacchelli, J.-B. Pomet, D. Prandi

Abstract— We propose an observer design for a 3-dimensional model of cortical activity dynamics in the visual cortex, under the measurement of the averaged activity. It is based on the construction of an embedding of the system into a triangular 4-dimensional system where the dynamics are not Lipschitz-continuous but bear Hölder-continuity properties allowing us to implement a sliding mode observer. We discuss stability of the convergence of the observer with respect to relevant perturbations and provide simulations illustrating the method.

I. Introduction

The introduction of control theory techniques to the field of neurosciences is a rich and challenging issue. Its many applications range from brain health monitoring [10] to brain-computer interfacing [11]. For instance, stabilization of signals in the brain via feedback control was used to alleviate Parkinson's disease symptoms [6]. Developing efficient and reliable strategies for online estimation of neural activity is fundamental to the implementation of such techniques. In the present paper, we focus on the question of observer design for a family of low dimensional neural fields. Neural fields equations model the evolution of the distribution of neuronal activity over a cortical domain. These dynamics are obtained by averaging the activity of large groups of neurons while maintaining spatial considerations in the interactions between neurons. Neural fields provide a powerful theoretical framework for studying brain activity (see [12] for a review on neural fields models in particular), and have proved their ability to replicate observed phenomena.

Neural fields models have a rich history of application to the study of the primary visual cortex V1 (see, e.g., [5] and references therein). In this paper, we are interested in a low-dimensional neural fields model of V1 discussed in [4], that we call Blumenfeld et al. model (see also [13]). The main feature of V1 that is captured by this model is the fact that neurons are more likely to be activated (or burst) when a stimulus arriving from the retina (through the LGN) is in accordance with some preset "preference" of each neuron. In particular, Blumenfeld et al. model focuses on orientation sensitivity, where edge orientation in the field of view induces neuron activation in V1 according to their prefered orientation. The favored orientation of a neuron is denoted by $\theta \in [-\pi/2, \pi/2)$, and their selectivity (how

A.M. Annabi, J.-B. Pomet, L. Sacchelli are with Université Côte d'Azur, Inria, CNRS, LJAD, France (email: adel-malik.annabi@inria.fr, jean-baptiste.pomet@inria.fr, ludovic.sacchelli@inria.fr)

D. Prandi is with Université Paris-Saclay, CNRS, CentraleSupélec, Laboratoire des Signaux et Systèmes, 91190, Gif-sur-Yvette, France (email: dario.prandi@centralesupelec.fr)

strong is that preference) with $r \in [0, \infty)$. This allows to label neurons in a given region of V1 according to the pair (θ, r), and to discard any other distinctive information. As a result, one can define the averaged post-membrane potential V for neurons with label (θ, r) (which we use as a substitute for neuronal activity), and describe its evolution with neural fields. Naturally, $V(\theta, r)$ must be π-periodic with respect to θ. Blumenfeld et al. model proposes to further reduce the dynamical model by focusing on the first few modes of the periodic function V, in order to detect the orientation corresponding to the highest activity in the considered region.

In that context, [1], by the authors of the present paper, discusses observability of the Blumenfeld et al. model from an control theory point of view. When the measurement is the post-membrane potential averaged over the whole region, as it happens with a non-localized electrode, we ask if it is possible to recover the most active orientation in the area. The analysis provided in [1] shows that this information is recoverable only under a persistent excitation condition. To test these conditions, the observability form was used to follow the standard high-gain observer design. This still required the introduction of a hybridization of the observer in order to cope with the observability singularities of the model, and limitations were imposed due to the Lipschitz-continuity failing in some regions. In the present paper, we discuss an observer design that is not based on the observability form, but rather on constructing an embedding of the dynamical model of Blumenfeld et al. that has triangular form and is such that the embedded dynamics are Hölder-continuous, allowing for the introduction of a sliding-mode observer design according to [3] (see also [8], [9]). Following these techniques yields convergence of the observer and also allows for a discussion of the stability of this convergence with respect to perturbation of the dynamics, that is extremely relevant in analyzing the behavior of this observer with respect to the reduction process on which the Blumenfeld et al. model is based.

II. Model discussion

Let us give an overview of the construction of the low-dimensional neural fields model from [4]. This discussion is developed further in [1]. We consider the evolution of the post-membrane potential V over an area of the cortex V1. Neurons of sensitivity $\theta \in [-\pi/2, \pi/2)$ and selectivity $r \in [0, +\infty)$ are grouped together. The distribution is assumed to be uniform in θ and to follow a (assumed to be known) probability distribution P in r. Without loss of generality for what follows, P is assumed to be compactly supported

in $[0, +\infty)$. Then according to the measure $\mu = \frac{P(r)}{\pi}\mathrm{d}r\mathrm{d}\theta$ over $\Omega = [0, +\infty) \times [-\pi/2, \pi/2]$, we define V as an $L^2_\mu(\Omega)$ function evolving in time according to a single-layer neural field equation

$$\begin{cases} \tau \dot{V}(t) = -V(t) + J \cdot \sigma(V(t)) + I_{\text{ext}}(t) \\ V(0) \in L^2_\mu(\Omega). \end{cases} \quad (1)$$

Here, $I_{\text{ext}} \in L^\infty(\mathbb{R}, L^2_\mu(\Omega)) \cap C^0(\mathbb{R}, L^2_\mu(\Omega))$ denotes the external input, $\tau > 0$ the temporal synaptic constant. The operator J models the global effect of neurons in Ω on neurons at (r, θ); it is given by a $L^2_{\mu \otimes \mu}$ integral kernel j over the domain Ω^2: $J \cdot U(r, \theta) = \int_\Omega j(r, \theta, r', \theta') U(r', \theta') \frac{P(r)}{\pi}\mathrm{d}r\mathrm{d}\theta$ for any $U \in L^2_\mu(\Omega)$. The firing rate function $\sigma : \mathbb{R} \to \mathbb{R}$ models how a population "charges" or "discharges" and is typically chosen to be a smooth sigmoidal function. Equation (1) is well defined and has a unique global solution for each initial condition $V(0) \in L^2_\mu(\Omega)$ which has the same regularity as I_{ext}. See [5], [13] for instance.

We make the following standard assumptions on the sigmoid function.

Assumption 2.1: The function σ is a $C^\infty(\mathbb{R}, \mathbb{R})$ function that is odd, strictly increasing (i.e., $\sigma' > 0$), convex-concave (i.e., $x\sigma''(x) \le 0$ for all $x \in \mathbb{R}$), and such that

$$\lim_{x \to -\infty} \sigma(x) = -1, \quad \lim_{x \to +\infty} \sigma(x) = 1,$$
$$\sigma(0) = 0, \quad \max_{\mathbb{R}} \sigma' = \sigma'(0).$$

Regarding the observation of V, we discussed in introduction the problem of estimation of V under the knowledge of the averaged potential V, so that

$$y = h(V(t)) = \int_\Omega V(r, \theta, t) \frac{P(r)}{\pi}\mathrm{d}r\mathrm{d}\theta. \quad (2)$$

Following the steps in [4], we assume that the interaction kernel j in operator J is of the form

$$j(r, \theta, r', \theta') = J_0 + J_1 rr' \cos(2(\theta - \theta')), \quad J_1 > 0, J_0 \ne 0.$$

This can be understood as a truncation of a Fourier expansion in $\theta - \theta'$ of $j(r, \theta, r', \theta') = J_0 + rr' j_1(\theta - \theta')$ with even j_1.

As $L^2_\mu(\Omega)$ splits into $\mathrm{range}(J) + \mathrm{range}(J)^\perp$, the projection on $\mathrm{range}(J)$ of any element $U \in L^2_\mu(\Omega)$ takes the form $U^\|(r, \theta, t) = u_0(t) + u_1(t) r \cos(2\theta) + u_2(t) r \sin(2\theta)$, $(u_0(t), u_1(t), u_2(t)) \in \mathbb{R}^3$ (with $U^\perp = U - U^\|$). Taking our input to be such that $I^\perp = 0$ yields that $V^\perp \to 0$ exponentially, which we will assume now to be equal to 0. We are therefore interested in the estimation of solutions V of (1) of the form $V = V^\|$.

Let us rewrite these dynamics in a manageable form. Letting, $i, j \in \mathbb{N}$, $\sigma^{(i)}$ be the i-th derivative of σ, we set the smooth functions

$$\Gamma^j_i(v_0, \rho) = \int_\Omega (r \cos 2\theta)^j \sigma^{(i)}(v_0 + \rho r \cos 2\theta) \frac{P(r)}{\pi}\mathrm{d}r\mathrm{d}\theta.$$

They have the following immediate properties (see [1]).

Lemma 2.2: The maps Γ^j_i satisfy the following points.
1) For all $i, j \in \mathbb{N}$, $\partial_{v_0}\Gamma^j_i = \Gamma^j_{i+1}$ and $\partial_\rho \Gamma^j_i = \Gamma^{j+1}_{i+1}$.
2) For any $v_0 \ne 0$, the function $\Gamma^0_0(v_0, \cdot)$ is injective.

3) For any $v_0 \ne 0$ and $\rho > 0$, we have $v_0 \Gamma^1_1(v_0, \rho) < 0$. Moreover, $\Gamma^1_1(v_0, 0) = 0$ for any $v_0 \in \mathbb{R}$.
4) For any $\rho \ge 0$, we have $\Gamma^0_0(0, \rho) = 0$.

Without loss of generality, we now assume $\tau = 1$. Letting $\bar{v} = (v_1, v_2)$, $\bar{I} = (I_1, I_2)$ and $v = (v_0, \bar{v})$, $\bar{I} = (I_0, \bar{I})$, the input-output formulation of Blumenfeld et al. model is

$$\begin{cases} \dot{v}_0 = -v_0 + J_0 \Gamma^0_0(v_0, |\bar{v}|) + I_0, \\ \dot{\bar{v}} = -\bar{v} + J_1 \Gamma^1_0(v_0, |\bar{v}|)\frac{\bar{v}}{|\bar{v}|} + \bar{I}, \\ y = v_0. \end{cases} \quad (3)$$

This expression is singular at $|\bar{v}| = 0$ but the singularity can be checked to be resolvable (and the dynamics to be smooth) thanks to Lemma 2.2. Assuming $I \in C^0([0, +\infty), \mathbb{R}^3)$, for any $v(0) \in \mathbb{R}^3$, solutions to the Cauchy problem are well defined for any positive time. Furthermore, under the assumption that $\sup_{[0, \infty)} |I| < \infty$, there exist $R^* > 0$ such that for any $R \ge R^*$ the ball $B_{\mathbb{R}^3}(0, R)$ is invariant by the dynamics. See [1, Proposition 2.4].

Next proposition sums up the observability analysis carried out in [1]; recall that differential observability means injectivity of the map $v(\cdot) \mapsto (y, \dot{y}, \dots)$.

Proposition 2.3: Assume the regularity $I \in C^3([0, +\infty), \mathbb{R}^3)$ for the input.
- If there exists $t_0 \in \mathbb{R}_+$ such that $y(t_0) = 0$, then (3) is not differentiably observable at t_0. More precisely, if $I_0 \equiv 0$ on an interval $[t_1, t_2] \subset \mathbb{R}_+$ then the system is not observable on that interval.
- Assume $I_0 \ge c > 0$. Then (3) is observable on $[t_1, t_2] \subset \mathbb{R}_+$ if and only if $\det\left(\bar{I}, \dot{\bar{I}}\right) \not\equiv 0$ on $[t_1, t_2]$.

The C^3-regularity of the input is mostly necessary to be able to differentiate the output 3 times and we will drop this assumption in the rest of the paper. The observability singularity at $y = 0$ has to be dealt with if we want to consider trajectories that can have vanishing output. The assumption $I_0 \ge c > 0$, motivated by the neuroscience modeling, ensures at most one crossing of the singularity $y = 0$. Our goal over the following sections is to describe an observer design for this system based on an embedding that puts (3) in a triangular form.

III. EMBEDDING AND TRIANGULAR FORM

For the remainder of the paper, we make the assumption that $I \in C^1([0, +\infty), \mathbb{R}^3)$, at least. Consider the mapping $\bar{G}_t : \mathbb{R}^4 \to \mathbb{R}^4$ defined for all $(v_0, \rho, \zeta) \in \mathbb{R} \times \mathbb{R} \times \mathbb{R}^2$ by

$$\bar{G}_t(v_0, \rho, \zeta) = \begin{pmatrix} x_0 \\ x_1 \\ x_2 \\ x_3 \end{pmatrix} = \begin{pmatrix} v_0 \\ J_0 \Gamma^0_0(v_0, \rho) \\ \langle \bar{I}, \zeta \rangle J_0 \Gamma^1_1(v_0, \rho) \\ \langle \dot{\bar{I}}, \zeta \rangle J_0 \Gamma^1_1(v_0, \rho) \end{pmatrix} \quad (4)$$

and $\Psi : \mathbb{R} \times (\mathbb{R}^2 \setminus \{0\}) \to \mathbb{R}^4$ defined by $\Psi(v_0, \bar{v}) = (v_0, |\bar{v}|, \bar{v}/|\bar{v}|)$. The embedding of (3) we wish to use is given by $G_t := \bar{G}_t \circ \Psi : \mathbb{R} \times (\mathbb{R}^2 \setminus \{0\}) \to \mathbb{R}^4$.

Lemma 3.1: Assume $|\det(\bar{I}, \dot{\bar{I}})| > 0$. For all $t > 0$, the map G_t can be continuously extended to $\mathbb{R}^* \times \mathbb{R}^2$ and is a smooth injection on this domain.

Proof: Denote $\rho = |\bar{v}|$. Extension of the domain of G_t to $\mathbb{R}^* \times \mathbb{R}^2$ comes from the fact that as $\rho \to 0$, for any $v_0 \neq 0$, $\Gamma_1^1(v_0, \rho) \sim \rho \Gamma_2^2(v_0, 0)$. Indeed $\Gamma_2^2(v_0, 0) \neq 0$ if and only if $v_0 \neq 0$. Hence G_t can be continuously extended at $(v_0, 0)$, for any v_0, by $G_t(v_0, 0) = (v_0, \Gamma_0^0(v_0, 0), 0, 0)$.

Injectivity of G_t is straightforward: assume $G(v) = G(\tilde{v})$, then $v_0 = \tilde{v}_0$. Denote $\tilde{\rho} = |\tilde{\bar{v}}|$. From Lemma 2.2, since $v_0 \neq 0$, $\rho = \tilde{\rho}$. Then since $\det(\bar{I}, \dot{I}) \neq 0$ and $\Gamma_1^1(v_0, \rho) \neq 0$ (from Lemma 2.2 again), we get $v = \tilde{v}$. ∎

In order to gain uniformity with respect to time of the modulus of continuity of the pseudo inverse of G_t that we will consider below, we assume the following.

Assumption 3.2: The input $I \in C^2([0, +\infty), \mathbb{R}^3)$, is bounded on $[0, +\infty)$, and so is $\dot{I}$. Furthermore, the following lower bounds hold for some positive numbers $c, \mu > 0$:

$$I_0(t) \geq c \text{ and } |\det(\bar{I}(t), \dot{I}(t))| \geq \mu, \quad \forall t \geq 0. \tag{5}$$

Set $\mathcal{D} = \{(x_0, x_1) \mid x_0 \neq 0, x_1 \in J_0 \Gamma_0^0(x_0, \mathbb{R})\}$ and for $0 < \delta < R$, set

$$\mathcal{D}_{\delta, R} = \{(x_0, x_1) \mid |x_0| \in [\delta, R], x_1 \in J_0 \Gamma_0^0(x_0, [-R, R])\}.$$

Relying on the previous lemma, we define for any given output y of (3) a pseudo inverse of G_t that extends the domain of G_t^{-1} beyond the image of G_t. First, we define a projection $\Pi : \mathbb{R}^4 \to \mathcal{D}_{\delta, R} \times \mathbb{R}^2$ that we assume to implicitly depend on the output y in the following way:

- $\Pi_2(x) = x_2, \Pi_3(x) = x_3$.
- If $y \geq 0$, then $\Pi_0(x)$ is the projection of x_0 on $[\delta, R]$, and $\Pi_1(x)$ is the projection of x_1 on $[J_0 \Gamma_0^0(\Pi_0(x), R), J_0 \sigma(\Pi_0(x))]$.
- If $y < 0$, then take $\Pi_0(x)$ as the projection of x_0 on $[-R, -\delta]$, while $\Pi_1(x)$ is the projection of x_1 on $[J_0 \sigma(\Pi_0(x)), J_0 \Gamma_0^0(\Pi_0(x), R)]$.

Then for any $x \in \mathbb{R}^4$, letting ρ be uniquely defined by $\Gamma_0^0(\Pi_0(x), \rho) = \Pi_1(x)/J_0$, we set $\mathcal{G}_t : \mathbb{R}^4 \times \mathbb{R} \to \mathbb{R}^3$

$$\mathcal{G}_t(x) = \left(\Pi_0(x), \frac{\rho}{J_0 \Gamma_1^1(\Pi_0(x), \rho)} \begin{pmatrix} I_1 & I_2 \\ \dot{I}_1 & \dot{I}_2 \end{pmatrix}^{-1} \begin{pmatrix} x_2 \\ x_3 \end{pmatrix} \right) \tag{6}$$

Remark 3.3: Having $\mathcal{G}_t$ depend on the sign of the output y is guided by the loss of injectivity of G_t in $\{v \in \mathbb{R}^3 \mid v_0 = 0\}$ (indicating loss of observability). This amounts to constructing two pseudo inverses on both $x_0 \geq 0$ and $x_0 < 0$ and picking the one most adapted to the measured output.

The pseudo inverse has been constructed to verify the following: for all $v \in \mathbb{R}^3$ such that $|v_0| \geq \delta, |v| \leq R$ and $v_0 y(t) > 0$ we have $\mathcal{G}_t(G_t(v)) = v$. We can prove that this extension of G_t^{-1} is uniformly continuous.

Lemma 3.4: Let $0 < \delta < R$. Under Assumption 3.2, there exist a class $\mathcal{K}$ function ω such that for every time $t \geq 0$, for every $(x, \tilde{x}) \in \mathbb{R}^4 \times \mathbb{R}^4$,

$$|\mathcal{G}_t(x) - \mathcal{G}_t(\tilde{x})| \leq \omega(|x - \tilde{x}|). \tag{7}$$

Proof: By definition we have $\Pi(x) \in \mathcal{D}_{\delta, R}$, and we can recover ρ from $\Pi(x)$. The maps Π_0, Π_1 being projections, they are 1-Lipschitz continuous. Furthermore, the function $\mathcal{G}_t$ is smooth in ρ: the singularity $\rho/\Gamma_1^1(\Pi_0(x), \rho)$

resolves again as $\Gamma_1^1(v_0, \rho) \sim \rho \Gamma_2^2(v_0, 0)$ (see Lemma 2.2). Hence $m : (x_0, x_1) \mapsto \frac{\rho}{J_0 \Gamma_1^1(\Pi_0(x), \rho)}$ is uniformly continuous and there exists ω', a class $\mathcal{K}$ function such that $|m(x_0, x_1) - m(\tilde{x}_0, \tilde{x}_1)| \leq \omega'(|x - \tilde{x}|)$. By Assumption 3.2, $a := \sup_{t \geq 0} \left\| \begin{pmatrix} I_1 & I_2 \\ \dot{I}_1 & \dot{I}_2 \end{pmatrix}^{-1} \right\| < \infty$. This implies that $|\mathcal{G}_t(x) - \mathcal{G}_t(\tilde{x})| \leq (1 + a)|x - \tilde{x}| + \omega'(|x - \tilde{x}|) =: \omega(|x - \tilde{x}|)$. ∎

We embed now system (3) by the application G_t to obtain a *triangular form*:

$$\begin{aligned} \dot{x}_0 &= x_1 + \phi_0(x_0, t) \\ \dot{x}_1 &= x_2 + \phi_1(x_0, x_1, t) \\ \dot{x}_2 &= x_3 + \phi_2(x_0, x_1, x_2, t) \\ \dot{x}_3 &= \phi_3(x_0, x_1, x_2, x_3, t). \end{aligned} \tag{8}$$

To implement a homogenuous sliding mode observer on the embedded domain, certain regularity conditions are required on the non-linearities ϕ_i (see [2], [3]), mainly, that there exist $\bar{b} > 0$ and $\alpha_{ij} \geq 0$ such that for all x, $\tilde{x}$ in $\mathbb{R}^4$ $|\phi_i(x_0, .., x_j, t) - \phi_i(\tilde{x}_0, .., \tilde{x}_j, t)| \leq \bar{b} \sum_{j=0}^i |x_j - \tilde{x}_j|^{\alpha_{ij}}$, with $\alpha_{i,j}$ verifying the conditions found in Table III. This is encapsulated in the following proposition.

$i \backslash j$	0	1	2	3
0	$\frac{3}{4}$			
$\alpha_{ij} \geq$ 1	$\frac{1}{2}$	$\frac{2}{3}$		
2	$\frac{1}{4}$	$\frac{1}{3}$	$\frac{1}{2}$	
3	0	0	0	0

TABLE I

HÖLDER RESTRICTIONS ON ϕ FOR A HOMOGENEOUS SLIDING MODE OBSERVER. SEE [2], [3].

Proposition 3.5: Suppose Assumption 3.2 holds. There exists continuous functions $\phi_0 : \mathbb{R} \times \mathbb{R} \to \mathbb{R}$, $\phi_1 : \mathcal{D} \times \mathbb{R} \to \mathbb{R}$, and $\phi_i : \mathcal{D} \times \mathbb{R}^{i-1} \times \mathbb{R} \to \mathbb{R}$, $i = 2, 3$, such that solutions of (3) have their image by G_t be solutions of (8).

Moreover, for $0 < \delta < R$ and K any compact subset of $\mathcal{D}_{\delta, R} \times \mathbb{R}^2$, the functions ϕ_0, ϕ_1 are Lipschitz-continuous and ϕ_2, ϕ_3 are $\frac{1}{2}$-Hölder-continuous uniformly in time. Mainly, they verify the conditions in Table III.

Proof: Let v be a solution of (3), and let $\rho = |\bar{v}|$, $\zeta = \bar{v}/|\bar{v}|$. Using the fact that for any $|v_0| > 0$ the mapping $\rho \to \Gamma_0^0(v_0, \rho)$ admits a smooth inverse on its image (see Lemma 2.2) and that due to Assumption 3.2, $\langle \ddot{\bar{I}}, \zeta \rangle J_0 \Gamma_1^1(v_0, \rho) = \alpha x_2 + \beta x_3$ with $\ddot{\bar{I}} = \alpha \bar{I} + \beta \dot{I}$ and α, β continuous function of time, basic calculations yields the expression of the different ϕ_i.

The proof of continuity can be resumed to solving the indeterminate form appearing in the expression of ϕ_2 and ϕ_3 when ρ is approaching zero, as all other terms are continuous. Omitting the variables in Γ_i^j, the indeterminate form is

$$\lim_{\rho \to 0} \frac{x_2^2}{J_0 \Gamma_1^1} \left(\frac{\Gamma_2^2}{\Gamma_1^1} - \frac{1}{\rho} \right)$$

From Lemma 2.2 and using that $\Gamma_i^j(v_0, 0) = 0$ when j is odd, developing the Taylor expansions when ρ is near zero yields $\Gamma_1^1(x_0, \rho) = \rho \Gamma_2^2(x_0, 0) + \rho^3 \Gamma_4^4(x_0, 0)/6 + o(\rho^4)$, we

deduce that $\frac{\rho\Gamma_2^2 - \Gamma_1^1}{\rho\Gamma_1^1} = \frac{\Gamma_4^4(x_0,0)}{3\Gamma_2^2(x_0,0)}\rho + o(\rho^2)$. This resolves the indeterminate form

$$\frac{x_2^2}{J_0\Gamma_1^1}\left(\frac{\Gamma_2^2}{\Gamma_1^1} - \frac{1}{\rho}\right) = \frac{x_2^2\Gamma_4^4(v_0,0)}{J_0 3\Gamma_2^2(x_0,0)^2} + o(\rho).$$

The only issue in terms of regularity comes from the functions Γ_i^j. The mapping $(v_0,\rho) \mapsto \Gamma_i^j(v_0,\rho)$ is smooth but the (inverse) mapping $(x_0,x_1) \mapsto (x_0,\rho)$ is not. Hence ϕ_i being smooth in ρ (at $\rho = 0$ included) is not sufficient to claim that the maps may be Hölder-continuous. For this, we prove that the inverse of $(x_0,\rho) \mapsto (x_0, J_0\Gamma_0^0(x_0,\rho))$ is locally $\frac{1}{2}$-Hölder-continuous.

Since $\Gamma_0^0(x_0,\cdot)$ is an even smooth function, we can define the odd smooth function

$$\gamma(x_0,s) := \text{sign}(s)\left(\Gamma_0^0(x_0,\sqrt{|s|}) - \Gamma_0^0(x_0,0)\right)$$

For any $\rho \geq 0$, the relation $x_1 - \Gamma_0^0(x_0,\rho) = 0$ can be extended to $m(x_0,x_1,s) = x_1 - \gamma(x_0,s) = 0$ for any $x_0, x_1 \in \mathcal{D}$, $s \in \mathbb{R}$. Then $\partial_s m = \Gamma_2^2(x_0,\sqrt{|s|}) > 0$ on $\mathcal{D} \times \mathbb{R}$. This allows to use the implicit function theorem to define $s(x_0,x_1)$ and to check that the Jacobian matrix $\|\text{Jac }s(x_0,x_1)\| \leq \frac{c}{\Gamma_2^2(|x_0|,\sqrt{|s(x_0,x_1)|})}$. Assuming $x \in K$, Γ_2^2 ends up lower bounded. Hence, applying the mean value theorem to γ, for any pair $(x_0,x_1),(\tilde{x}_0,\tilde{x}_1)$ and associated $\rho, \tilde{\rho}$, one has $|\rho^2 - \tilde{\rho}^2|^2 \leq C(|x_0 - \tilde{x}_0|^2 + |x_1 - \tilde{x}_1|^2)$. Since $|\rho - \tilde{\rho}|^2 \leq |\rho^2 - \tilde{\rho}^2|$ (as they're both non-negative), this concludes the Hölder-continuity proof. From this we deduce that ϕ_i, $i = 2, 3$ are all $\frac{1}{2}$-Hölder-continuous as functions of (x_0,x_1,x_2,x_3) in restriction to the compact K, uniformity in time is immediate from Assumption 3.2. Finally, Lipschitz-continuity of $\phi_1(\cdot,t)$ is straight-forward, as it can be seen as a smooth function of ρ^2, shown above to be a Lipschitz-continuous function of (x_0,x_1). ∎

IV. OBSERVER DESIGN

In this section, we propose an observer for system (3) and prove its main properties.

Let v be a solution of (3) with output y. We consider the following hybrid observer:

$$\begin{cases} \text{If } |y(t)| > \delta : \\ \hat{v}(t) = \mathcal{G}_t(\hat{x}(t)), \begin{cases} \dot{\hat{x}}_0 = \hat{\phi}_0 + \hat{x}_1 - Lk_0\lceil\hat{x}_0 - y\rceil^{\frac{3}{4}} \\ \dot{\hat{x}}_1 = \hat{\phi}_1 + \hat{x}_2 - L^2 k_1\lceil\hat{x}_0 - y\rceil^{\frac{1}{2}} \\ \dot{\hat{x}}_2 = \hat{\phi}_2 + \hat{x}_3 - L^3 k_2\lceil\hat{x}_0 - y\rceil^{\frac{1}{4}} \\ \dot{\hat{x}}_3 \in \hat{\phi}_3 - L^4 k_3\text{sign}(\hat{x}_0 - y). \end{cases} \\ \text{If } |y(t)| < \delta : \\ \dot{\hat{v}}(t) = f(\hat{v},t), \ \hat{x}(t) = G_t(\hat{v}(t)), \end{cases}$$ (9)

where f indicates the right-hand side of (3); L, k_i and δ are parameters to be tuned. For $z \in \mathbb{R}$, and $\alpha > 0$, we denoted $\lceil z\rceil^\alpha := \text{sign}(z)|z|^\alpha$, with $\text{sign}(z)$ the set valued mapping

$$\text{sign}(z) := \begin{cases} \{1\} & \text{if } z > 0, \\ [-1,1] & \text{if } z = 0, \\ \{-1\} & \text{if } z < 0. \end{cases}$$

With $M = 2|J_0|\sup_{\mathcal{D}_{\delta,R}}|\Gamma_1^1|$, $M_2 = M\sup_{\mathbb{R}_+}\|\bar{I}\|$ and $M_3 = M\sup_{\mathbb{R}_+}\|\dot{\bar{I}}\|$, we set $K = \mathcal{D}_{\delta,R} \times [-M_2,M_2] \times [-M_3,M_3]$. The functions $\hat{\phi}_i$ are saturated versions of the functions ϕ_i, defined by $\hat{\phi}_i = S_i \circ \phi_i \circ d_i \circ \Pi(x)$ for $i = 0,1,2,3$, with $S_i(z)$ the projection of $z \in \mathbb{R}$ onto $[-\sup_{x\in K}|\phi_i(x)|, \sup_{x\in K}|\phi_i(x)|]$, and $d_i(x) = (x_0, \ldots, x_i)$.

Remark 4.1: Projection Π ensures maps ϕ_i get restricted to $\mathcal{D}_{\delta,R} \times \mathbb{R}^2$ where they are well defined and verify the Hölder-conditions of Table III on any sub-compact. Saturations S_i are added because $B_{\mathbb{R}^3}(0,R)$ is an invariant attracting ball if $R > 0$ is sufficiently large and that $G_t(B_{\mathbb{R}^3}(0,R)) \subset K$ under Assumption 3.2. From [2, Lemma A.2.2] and the Lipschitz-continuity of Π uniformly in time ensures that $\hat{\phi}$ maintain Proposition 3.5 for every pair $(x,\hat{x}) \in K \times \mathbb{R}^4$.

Observer (9) operates as a hybrid system, transitioning between two dynamical systems based on the sign of $|y(t)| - \delta$. It involves states $\hat{x} \in \mathbb{R}^4$ and $\hat{v} \in \mathbb{R}^3$. The first dynamical system is a differential inclusion and is to be understood in the Fillipov sense [7]. It is (8), with output $y = x_0$ and trajectories remaining in K (in particular $|x_0| > \delta$). This includes trajectories $x(t) = G_t(v(t))$ with v solution of (3). Assume at some t_1, $|y(t)| - \delta$ switches from positive to negative. Then we switch the role of $\hat{v}$ and $\hat{x}$: $\hat{v}$ is continued by following the dynamics of (3) with initial value at t_1^+ given by $\mathcal{G}_{t_1^-}(\hat{x}(t_1^-))$. The same operation is reversed if at some t_2, $|y(t)| - \delta$ switches from negative to positive. Under Assumption 3.2, this piecewise definition is guaranteed to be well posed (no Zeno effect). Indeed, from [1, Proposition 3.2], solutions v of (3) have v_0 strictly increasing near 0. In other words, there exists $\delta^* > 0$ such that trajectories remain in $\{v \in \mathbb{R}^3, |v_0| \leq \delta\}$ for a finite (and tunable) time t_δ when $\delta \leq \delta^*$. We note by $t_1 := \inf\{t \geq 0; y(t_1) = -\delta\}$ and $t_2 := \inf\{t \geq 0; y(t_2) = \delta\}$ the two possible switching time under Assumption 3.2. The value of δ^* is computed in [1, Proposition 3.4], we leave it as a black box here.

Regarding the existence of global solutions of (9) we can say what follows. The set valued function $\text{sign}(\cdot)$ is upper-semi continuous, has convex and compact values. From Proposition 3.5 and Remark 4.1, as well as [7], we deduce that there exist absolutely continuous solutions to the first half of (9), that we denote $\hat{z}(t)$ (abusing notations for simplicity). The same is true for the second equation as f is globally Lipschitz. The absolute continuity of $\mathcal{G}$ and G implies that of $\hat{v}$ and $\hat{x}$ respectively on each side. From [1, Proposition 3.2], there exist $\delta^* > 0$ such that if $\delta < \delta^*$ there exists at most two times $t_2 > t_1 \geq 0$ such that $y(t_1) = -\delta$ and $y(t_2) = \delta$. Hence, $\hat{v}$ and $\hat{z}$ are globally defined piece-wise continuous. The construction of $\mathcal{G}$ as a pseudo inverse (6) implies global continuity of $\hat{v}$ and at most one jump for $\hat{z}$. This is encapsulated in the following.

Proposition 4.2: Suppose Assumption 3.2 holds. There exists $\delta^* > 0$ such that for any $\delta < \delta^*$, (9) admits globally defined piecewise continuous solutions (denoted $\hat{v}$ and $\hat{x}$).

We can now state the main convergence result of this paper

Theorem 4.3: Suppose Assumption 3.2 holds. Let $0 < \delta < \delta^*$. There exist gains $k_i > 0$ and $L^* > 0$ such that for every $L \geq L^*$ there exists a class $\mathcal{KL}$ function $\mathcal{B}$ such that for every solutions of (9) initialised with $\hat{v}(0) \in B_{\mathbb{R}^3}(0, R)$, $\hat{z}(0) = G_0(\hat{v}(0))$ we have

$$|v(t) - \hat{v}(t)| \leq \mathcal{B}(|v(0) - \hat{v}(0)|, t), \ t \geq t_\delta, \quad (10)$$

with $t_\delta > 0$ depending only on δ, introduced in [1, Proposition 3.2]. We recall that t_δ is an upper bound of $t_2 - t_1$ above, and such that $t_\delta \to 0$ as $\delta \to 0$.

Proof: We denote by $x(t) = G_t(\bar{v}(t))$ for $t \geq 0$. Let $S := \{t \geq 0, |y(t)| \leq t_\delta\}$. From [1, Proposition 3.2], either $S = [t_1, t_2]$, $0 \leq t_1 \leq t_2 \leq t_1 + t_\delta$, or $S = \emptyset$, in which case we say $t_1 = \infty$. From Proposition 4.2, we are assured that trajectories $\hat{v}$ and $\hat{x}$ are defined globally when $\delta < \delta^*$. We denote by $L_1 > 0$ and $L_2 > 0$ Lipschitz constants (uniform in time for L_1) of, respectively, G_t and f on $\mathbb{R}^3$.

We describe first the error during each phase of the hybrid system. When $|y| \geq \delta$ and x remains in to K, we are in position to apply [3, Proposition 4] which gives the existence of gains k_i and L^* and a class $\mathcal{KL}$ function $\mathcal{B}_1$ such that for any interval $[t_0, t_f]$ where $|y(t)| \geq \delta$, for all $t \in [t_0, t_f]$

$$|\hat{z}(t) - z(t)| \leq B_1(|\hat{x}(t_0) - x(t_0)|, t - t_0), \quad (11)$$

(we omit the fact t_0 may be a switching time, in which case t_0^+ should be employed). Using then Lemma 3.4 and Remark 4.1, we have for all $t \in [t_0, t_f]$

$$|\hat{v}(t) - v(t)| \leq \omega \circ B_1(|\hat{x}(t_0) - x(t_0)|, t - t_0). \quad (12)$$

If $t_0 = t_2$, i.e., we are at a switching time, then from $\hat{z}(t_2^+) = G_{t_2^-}(\hat{v}(t_2^-))$ we get for $t \in [t_0, t_f]$

$$|\hat{v}(t) - v(t)| \leq \omega \circ B_1(L_1|\hat{v}(t_0) - v(t_0)|, t - t_0). \quad (13)$$

Using Grönwall's lemma, the error for $t \in S$ is given by

$$|\hat{v}(t) - v(t)| \leq e^{L_2 t_\delta}|\hat{v}(t_1) - v(t_1)|. \quad (14)$$

We now prove the existence of a global class $\mathcal{KL}$ function as stated. Consider two cases: $t_1 = 0$ and $t_1 > 0$ ($t_1 = \infty$ is similar to $t_1 = 0$). In the first case, we are assured that (13) holds for $t_0 = t_2$ and $t_f = \infty$ and (14) for $t_0 = 0$ and $t_f = t_2$. Combining the two yields for all $t \geq t_\delta$

$$|\bar{v}(t) - \hat{v}(t)| \leq \omega \circ B_1(L_1 e^{L_2 t_\delta}|\hat{v}(0) - v(0)|, t - t_\delta), \quad (15)$$

which is a $\mathcal{KL}$ function as ω is a $\mathcal{K}$ function as in Lemma 3.4. Up to taking $L_1 \geq 1$, we denote $B_2 := \omega \circ B_1(L_1 e^{L_2 t_\delta} \cdot, \cdot)$. One can easily check that we can extend B_2 into a new $\mathcal{KL}$ function $\bar{\mathcal{B}}$ such that it verifies the wanted point in this case.

Consider now the second case $t_1 > 0$. Combining (13) and (14) yields for all $t \geq 0$

$$|v(t) - \hat{v}(t)| \leq \omega \circ \mathcal{B}'(|v(0) - \hat{v}(0)|, t, t_2), \quad (16)$$

with $\mathcal{B}'(r, t, t_2)$ given by either of three cases:

$$\begin{cases} B_1(r, t) & \text{if } 0 \leq t \leq t_2 - t_\delta, \\ L_1 e^{L_2(t - t_2 + t_\delta)} B_1(r, t_2 - t_\delta) & \text{if } t_2 - t_\delta \leq t \leq t_2, \\ B_1(B_2(r, t_2 - t_\delta), t - t_2) & \text{if } t > t_2. \end{cases} \quad (17)$$

(We used the $\mathcal{KL}$ character of B_1, B_2 to condense dependence in t_1 and t_2 into a dependence in t_2 of the upper bound.) To conclude, we prove that $\bar{\mathcal{B}}'(r, t) := \sup_{t_2 \geq 0} \mathcal{B}'(r, t, t_2)$ is a $\mathcal{KL}$ function. Continuity and growth are immediate, let us check that $\lim_{t \to \infty} \bar{\mathcal{B}}'(r, t) = 0$. We prove it by hand. Fix $r, \varepsilon > 0$. There exists A such that

$$L_1 e^{L_2 t_\delta} B_1(r, A - t_\delta) \leq \varepsilon, \quad (18)$$
$$B_1(B_2(r, A - t_\delta), 0) \leq \varepsilon, \quad (19)$$
$$B_1(B_2(r, 0), A) \leq \varepsilon. \quad (20)$$

Take $t \geq 2A$. If $t_2 \geq 2A$ (18) implies that $\mathcal{B}'(r, t, t_2) \leq \varepsilon$, if $A \leq t_2 \leq 2A$, (19) implies that $\mathcal{B}'(r, t, t_2) \leq \varepsilon$, and finally if $t_2 \leq A$, (19) implies the same. Hence if $t \geq 2A$, $\bar{\mathcal{B}}'(r, t) \leq \varepsilon$. We conclude by taking $\mathcal{B} := \sup\{\bar{\mathcal{B}}', \bar{\mathcal{B}}\}$. ∎

V. INPUT-OUTPUT STABILITY DISCUSSION

Since our observer is a reduced model of the infinite dimensional (1) (see Section II) and because other disturbances naturally occur, we present in this section a discussion of the behavior of the observer (9) in presence of bounded disturbances $w = (w_0, w_1, w_2) \in L^\infty(\mathbb{R}_+; \mathbb{R}^3)$ on the dynamics, and $\nu \in L^\infty(\mathbb{R}_+; \mathbb{R})$ on the measurement, which verify respectively the Caratheodory conditions. In their presence, System (3) becomes

$$\begin{cases} \dot{v}_0 = -v_0 + J_0 \Gamma_0^0(v_0, |\bar{v}|) + I_0 + w_0, \\ \dot{\bar{v}} = -\bar{v} + J_1 \Gamma_0^1(v_0, |\bar{v}|)\frac{v}{|\bar{v}|} + \bar{I} + \bar{w}, \\ y = v_0 + \nu, \end{cases} \quad (21)$$

with $\bar{w} = (w_1, w_2)$. Propagating through the embedding G_t, they also appear linear in the pertubation of (8), that becomes

$$\dot{x}_i = \phi_i(x_0, ..., x_i, t) + x_{i+1} + \hat{w}_i, \quad (22)$$

with $\tilde{w}_i(t) := (\partial_v G_t(v)w)_i$, which is uniformly bounded.

As the switching condition in (9) depends on the output of the system, for large disturbances on the output, Zeno phenomena may appear and the observer fails. However, it possesses some robustness to "small" disturbances. Indeed, if there exist $\bar{c} > 0$ such that $I_0 - \|w_0\|_{L^\infty} > \bar{c}$ then from (21), using that $|\Gamma_0^0(v_0, |\bar{v}|)| \geq -\sigma(v_0)$ in the dynamics of v_0 yields that there exist $\bar{\delta}^* > 0$ such that if $|v_0| < \delta^*$, then the derivative v_0 is strictly positive. Then, assuming $\|\nu\|_{L^\infty} < \frac{\bar{\delta}^*}{2}$, for any solution of (21) if $\|\nu\|_{L^\infty} < \frac{\bar{\delta}^*}{2}$, it holds that there is a time $t' \geq 0$ such that $|v_0(t') + \nu(t')| < \frac{\bar{\delta}^*}{2}$ then $v_0(t) + \nu(t) \geq \frac{\bar{\delta}^*}{2}$ for each time $t \geq t' + t_{\frac{\bar{\delta}^*}{2}}$, with $t_{\frac{\bar{\delta}^*}{2}}$ given by the expression in [1, Proposition 3.2].

We define $\bar{t}_1 := \inf\{t \geq 0, y(t) \geq -\frac{\bar{\delta}^*}{2}\}$ and $\bar{t}_2 := \inf\{t \geq 0, y(t) \geq \frac{\bar{\delta}^*}{2}\}$. For any trajectory v of (21) such that $\bar{t}_1 = 0$, we follow the same idea as in the proof of Theorem 4.3. In particular, [3, Proposition 4] ensures the input to state stability property for the x-observer in (9). This requires the same condition as above, mainly $I_0 - \|w_0\|_{L^\infty} > \bar{c}$ and $\|\nu\| < \frac{\bar{\delta}^*}{2}$. Therefore, there exist $\bar{\mathcal{B}}_1$, a $\mathcal{KL}$ function, and $\gamma(\cdot, \cdot)$, a $\mathcal{K}$ function in each variable, such that

$$\begin{aligned} |\hat{x} - x| &\leq \bar{\mathcal{B}}_1(|e(0)|, t) + \gamma(\|w\|_\infty, \|\nu\|_\infty), \\ |\hat{v} - v| &\leq \omega\left(\bar{\mathcal{B}}_1(|e(0)|, t) + \gamma(\|w\|_\infty, \|\nu\|_\infty)\right). \end{aligned} \quad (23)$$

The most problematic cases arise when $\bar{t}_1 > 0$. For any time $t \geq 0$ in the switch interval $[\bar{t}_1, \bar{t}_2]$, one can obtains

$$|\hat{v}(t) - v(t)| \leq e^{L_2(t-\bar{t}_1)}|\hat{v}(\bar{t}_1) - v(\bar{t}_1)| + \|w\|_\infty/L_2,$$
$$|\hat{x}(t) - x(t)| \leq L_1 e^{L_2(t-\bar{t}_1)}\omega(\bar{\mathcal{B}}_1(|e(0)|, t_1) \quad (24)$$
$$+ \gamma(\|w\|_\infty, \|\nu\|_\infty)) + \|w\|_\infty/L_2$$

with $\bar{t}_2 - \bar{t}_1 \leq \frac{\bar{\delta}^*}{2}$. Let $C(t, e(0), t_1, w, \nu)$ denote the right hand side of the previous relation. We can then treat the situation after the switching time $\bar{t}_2$ by adapting (23). Again, from the same proposition in [3], we have for $t \geq t_2$

$$|\hat{x}(t) - x(t)| \leq \bar{\mathcal{B}}_1(|C(t_2^-, e(0), \bar{t}_1, w, \nu)|, t-\bar{t}_2) + \gamma(\|w\|, \|\nu\|)).$$
$$(25)$$

The estimation of $|\hat{v}(t) - v(t)|$ for $t \geq \bar{t}_2$ can then be obtain by applying ω to (25), and using $|e(0)| \leq L_1|\hat{v}(0) - v(0)|$.

This description of the bound of the error is preliminary and doesn't fully answer the modelization questions raised in the beginning of the section. Nevertheless, when the only source of model noise comes from the fact that $V^\perp(0) \neq 0$, since $V^\perp$ converges to 0, equations (23)-(24)-(25) yield that convergence of the observer is still true.

VI. NUMERICAL SIMULATIONS

We propose a numerical simulation for the observer (9) with parameters chosen as follows: $J_0 = -1$, $J_1 = 1.5$, and $\sigma = \tanh(\mu \cdot)$ with $\mu = 10$. The distribution P is set as the Dirac mass $P = \delta_{r=1}$ (see [13]). The input is $I_0(t) = \varepsilon(1-\beta)$ and $\bar{I}(t) = \beta\varepsilon\left(\cos(\frac{2\pi}{10}t), \sin(\frac{2\pi}{10}t)\right)$, with $\beta = 10^{-1}$ and $\varepsilon = 10^{-1}$. The initial condition $v(0) = (-6, 2.5, -2)$ ensures $y(0) < -\delta$ to trigger the switching mechanism.

We set the relaxation time constant $\tau = 5$ (for better illustration of error growth during the switch) and the observer's initial condition $\hat{v}(0) = (-0.01, 2, -1)$, $\hat{x}(0) = G_0(\hat{v}(0))$. With $J_0 < 0$, we chose $\delta = 0.7$ (see [1]). Gains k_i follow [3], [8], with $L = 3$. We employed an explicit Euler scheme with a step size of 10^{-5} over the interval $[0, 9]$. Trajectories are shown on the immersed domain for clarity. Figure 1 presents the error $\|e\| = \|\hat{x}(t) - x(t)\|$ in log scale, and Figure 2 highlights the error dynamics before the switch.
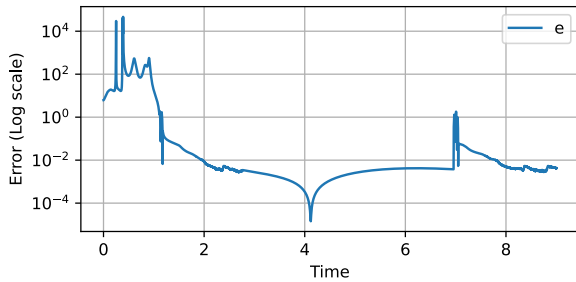

Fig. 1. Plot of the error $\|e\|$ in log scale. The trajectories v were initialized with $v(0) < -\delta$. Switching occurs at $t_1 \approx 2.5$ and $t_2 \approx 6.5$. Peaking phenomena are observed at the start and at t_2, where the sliding mode observer in x restarts. Since the error peaking at t_2 is proportional to the error at t_1, the peak is significantly smaller the second time, highlighting the advantage of the hybrid system and the homogeneous observer. At t_1, the sliding mode observer is turned off, and v and $\hat{v}$ follow neural field dynamics. States x and $\hat{x}$ are tracked via the mapping G, causing error drift over $[t_1, t_2]$.
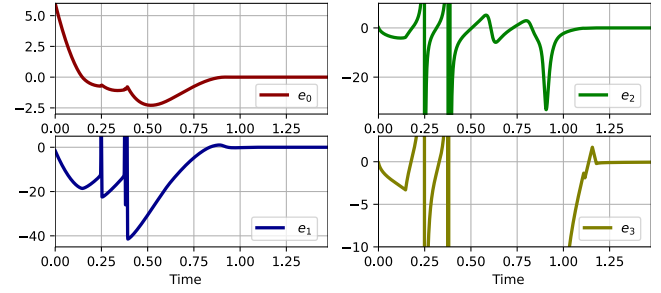

Fig. 2. Error $e(t) = x(t) - \hat{x}(t)$ before the switching time t_1. We see the sliding effect on the trajectory e_4 in the bottom graph and the overall finite time convergence.

VII. CONCLUSION

In this article, we presented the observer (9) which ensures finite-time convergence for solutions of (3) and discussed its stability. It is an enhanced version of the observer introduced in our previous work [1] which demonstrated asymptotic convergence only for specific solutions that were deemed biologically relevant. Key advancements were made in the construction of the immersion yielding (8) and its pseudo-inverse. Note that the hybrid design leaves some flexibility in changing the choice of the observer on the immersed domain, as long as it deals with the Hölder regularity of the non-linearities in (8) and achieves asymptotic convergence.

REFERENCES

[1] A. M. Annabi, J.-B. Pomet, D. Prandi, and L. Sacchelli. Activity estimation via distributed measurements in an orientation sensitive neural fields model of the visual cortex. *arXiv:2403.01906*, 2024.
[2] P. Bernard. *Observer design for nonlinear systems*, volume 479. Springer, 2019.
[3] P. Bernard, L. Praly, and V. Andrieu. Observers for a non-Lipschitz triangular form. *Automatica*, 82:301–313, 2017.
[4] B. Blumenfeld, D. Bibitchkov, and M. Tsodyks. Neural network model of the primary visual cortex: from functional architecture to lateral connectivity and back. *Journal of computational neuroscience*, 20:219–241, 2006.
[5] P. C. Bressloff. Spatiotemporal dynamics of continuum neural fields. *Journal of Physics A: Mathematical and Theoretical*, 45(3), 2011.
[6] G. I. Detorakis, A. Chaillet, S. Palfi, and S. Senova. Closed-loop stimulation of a delayed neural fields model of parkinsonian stn-gpe network: a theoretical and computational study. *Frontiers in neuroscience*, 9:237, 2015.
[7] A. F. Filippov. *Differential Equations with Discontinuous Righthand Sides*, volume 18 of *Mathematics and Its Applications*. Springer Netherlands, Dordrecht, 1988.
[8] A. Levant. Higher-order sliding modes, differentiation and output-feedback control. *International Journal of Control*, 76(9-10):924–941, 2003.
[9] C. Qian. A homogeneous domination approach for global output feedback stabilization of a class of nonlinear systems. In *Proceedings of the 2005, ACC, 2005.*, pages 4708–4715 vol. 7, 2005.
[10] M. Sood, P. Besson, M. Muthalib, U. Jindal, S. Perrey, A. Dutta, and M. Hayashibe. Nirs-eeg joint imaging during transcranial direct current stimulation: online parameter estimation with an autoregressive model. *Journal of neuroscience methods*, 274:71–80, 2016.
[11] E. Sorrell, M. E. Rule, and T. O'Leary. Brain–machine interfaces: Closed-loop control in an adaptive system. *Annual Review of Control, Robotics, and Autonomous Systems*, 4:167–189, 2021.
[12] J. R. Terry, W. Woldman, A. D. Peterson, and B. J. Cook. Neural field models: A mathematical overview and unifying framework. *Mathematical Neuroscience and Applications*, 2, 2022.
[13] R. Veltz and O. Faugeras. Local/global analysis of the stationary solutions of some neural field equations. *SIAM Journal on Applied Dynamical Systems*, 9(3):954–998, 2010.